J. Phys. I France **5** (1995) 111–127 JANUARY **1995**, PAGE 111

Classification
Physics Abstracts
61.10 — 61.40M — 68.55

Line-Shape Analysis of High Resolution X-Ray Diffraction Spectra of Finite Size Thue-Morse GaAs-AlAs Multilayer Heterostructures

Jacques Peyrière([1]), Eric Cockayne([2]) and Françoise Axel([2])

([1]) Equipe d'Analyse Harmonique(*), Bât. 425, Université Paris-Sud, 91405 Orsay, France
([2]) Laboratoire de Physique des Solides(**), Bât. 510, Université Paris-Sud, 91405 Orsay, France

(Received 15 July 1994, received in final form 12 September 1994, accepted 26 September 1994)

Abstract. — We present a detailed and thorough theoretical and numerical line shape analysis of high resolution X-ray diffraction spectra of Thue-Morse GaAs-AlAs superlattice heterostructures having finite size (2^n layers), which fully confirms the essentials of the preliminary analysis of previous work [1]: Most of the peaks are labeled by the irreducible rationals $k/(3.2^m)$, k and m integers, in convenient units, the dependence of their intensity on sample size is governed by exponents $\alpha_n(q)$, $0 < \alpha_n(q) < 2$ and the diffraction spectrum retains the essential properties of a singular continuous measure. The effects of instrumental parameters is taken into account, in particular detector resolution effects. Furthermore we investigate the effects on the diffraction spectrum of MBE deposited layer roughness, represented by a random fluctuation of layer thickness.

1. Introduction

The discovery of quasicrystals has shown the importance, for the description of long range order in solids, of ordered non-crystalline structures, some of which show new and surprising symmetries [2]. In particular, natural or model systems exhibiting quasiperiodicity have focused interest on geometric order beyond standard periodicity and quasiperiodicity, such as the order inherent in algorithmic (substitutional or automatic) sequences in one or more dimensions.

In previous work [1], one of us presented a preliminary analysis of high resolution X-ray diffraction spectra of GaAs-AlAs superlattice heterostructures composed of $N \equiv 2^n$ such layers arranged according to the Prouhet Thue-Morse (PTM) sequence. Here we present a detailed theoretical and numerical analysis of these data, which fully confirms the previous description of the principal features of the spectrum.

(*) CNRS - URA 757.
(**) CNRS - URA 002.

After briefly recalling some relevant properties of the PTM sequence (Sect. 2) and the essential features of the experimental situation (Sect. 3) we present in Section 4 the calculation of the diffraction amplitude $\hat{S}_n(q)$ for a multilayer sample of length $L = 2^n d$ and the analysis of the properties of the experimental X-ray spectrum, which we also numerically calculate. Then in Section 5, we study the effects on the spectrum of layer surface roughness, represented by a random fluctuation of layer thickness.

2. The Prouhet-Thue-Morse Abstract Sequence

We summarize some properties of the Prouhet-Thue-Morse (PTM) sequence $\{\varepsilon_j\}$ [3-5] which will be useful later on.

The PTM sequence can be defined

1) by the action of a substitution σ on a two letter alphabet, e.g. $(+1, -1)$ or $(1, 0)$ with a choice of initial conditions

$$\sigma \begin{pmatrix} 0 \to 0 & 1 \\ 1 \to 1 & 0 \end{pmatrix} \quad \text{or} \quad \begin{pmatrix} 1 \to & 1 & -1 \\ -1 \to & -1 & 1 \end{pmatrix} \tag{1}$$

The result of the first iterations with alphabet (0, 1) and $\varepsilon_0 = 0$ yields:

0
01
0110
01101001
0110100110010110 etc.

2) recursively by

$$\begin{matrix} \begin{cases} \varepsilon_{2n} = \varepsilon_n \\ \varepsilon_{2n+1} = 1 - \varepsilon_n \end{cases} \\ \text{alphabet } (0,1) \end{matrix} \quad \text{or} \quad \begin{matrix} \begin{cases} \varepsilon_{2n} = \varepsilon_n \\ \varepsilon_{2n+1} = -\varepsilon_n \end{cases} \\ \text{alphabet } (1,-1) \end{matrix} \quad \text{for all } n > 0 \tag{2}$$

from which follows:

$$\varepsilon_{2^n+j} = 1 - \varepsilon_j \quad (\text{or } \varepsilon_{2^n+j} = -\varepsilon_j) \text{ for } 0 \leq j < 2^n \tag{3}$$

3) using a 2-automaton. The reader is referred to references [6-9] for more details. We use in each Section whichever alphabet [(0, 1) or (1, −1)] is more convenient, and use corresponding subscripts for physical quantities. Let

$$s_j = \sum_{0 \leq k < j} \varepsilon_k \tag{4}$$

Trivially, with the alphabet (1, −1)

$$\begin{aligned} s_{2j} &= 0 \\ s_{2j+1} &= \varepsilon_{2j} = \varepsilon_j \end{aligned} \tag{5}$$

the number of sites
- with $\varepsilon_k = +1$ in a sequence having a total of j sites is $(j + s_j)/2$,
- with $\varepsilon_k = -1$ in a sequence having a total of j sites is $(j - s_j)/2$

Therefore a heterostructure with j layers of two types of thickness d_1 and d_{-1} arranged according to the PTM sequence has length

$$x_j = \sum_{0 \leq k < j} d_{\varepsilon_k} = \frac{j + s_j}{2} d_1 + \frac{j - s_j}{2} d_{-1} \tag{6}$$

It is known that the symbolic dynamical system associated with the PTM substitution has a singular continuous spectrum.

Indeed, the Fourier Transform

$$\hat{\varepsilon}_n(q) = \sum_{j=0}^{2^n-1} \varepsilon_j \exp(-2i\pi jq) \tag{7}$$

where $\{\varepsilon_j\}$ is the PTM sequence on the alphabet $(1, -1)$ beginning with 1 is [10-12, 27]

$$\hat{\varepsilon}_n(q) = \prod_{0\leq j<n} \left(1 - \mathrm{e}^{-2i\pi q 2^j}\right) \tag{8}$$

Therefore,

$$|\hat{\varepsilon}_n(q)|^2 = 2^n \prod_{0\leq j<n} \left(1 - \cos 2\pi q 2^j\right) \tag{9}$$

and the sequence of measures $2^{-n}|\hat{\varepsilon}_n(q)|^2 \mathrm{d}q$ converges towards a measure ν singular with respect to the Lebesgue measure [29]. Using Wiener's criterion, the measure ν can be shown to be continuous (for an account of the Lebesgue decomposition of measures, see, for instance [13]). When the $(0, 1)$ alphabet is used instead, a supplementary term proportional to the Dirac distribution at the origin appears [12].

3. Materials and Methods

They were described in [1, 15, 17, 18]. Samples having $N = 2^n$ layers with $n = 7$ and 10 were obtained by molecular-beam epitaxy (MBE) deposition on GaAs (001) substrate. The two types of layers made of GaAs (resp. AlAs) were arranged according to the binary Prouhet-Thue-Morse (PTM) sequence. Each was composed of 5 units of the relevant cubic crystalline lattice ("zinc blende" for both) with lattice constant a_0 (resp. a_1), with thickness $d_0 = n_0 a_0 = 5a_0$ (resp. $d_1 = n_1 a_1 = 5a_1$). Such samples were made for the first time in 1987 [19]. The Fibonacci case had been investigated before [14-18].

The high resolution measurements of the X-ray diffraction pattern of Figure 2 of reference [1] were made with Cu Kα_1 radiation. A monochromator of GaAs (111) and an analyser of Si (111) were used. The resolution is so high that the (004) reflection of the grown crystal and of the GaAs substrate are separated. The detailed procedure of the measurement is nearly the same as that of the measurement for the Fibonacci lattices and has been described elsewhere [15, 17, 18].

4. Calculation of the Diffraction Amplitude and Analysis of the Spectrum

We proceed to calculate the diffraction spectra of the multilayer, using a description accurate at the atomic scale. Studies of the Fourier Transforms of various deterministic sequence have been published before [26-28, 30, 31] . Each layer of GaAs (resp. AlAs) contains $2n_0$ (resp. $2n_1$) planes of Ga (resp. Al) and $2n_0$ (resp. $2n_1$) As planes. Normally the spacing between an As plane and a Ga (resp. Al) plane is $a_0/4$ (resp. $a_1/4$), except perhaps at the contact between two different layers where this is a first order approximation (A third length, a_2 probably closer to $(a_0 + a_1)/2$ should in fact be introduced; in this work, we limit ourselves to a two-length approximation).

Let $f_{As}(q)$, $f_{Ga}(q)$, $f_{Al}(q)$ be the atomic structure factors as a function of the wave vector q and define $d = (d_0 + d_1)/2$ and $a = (a_0 + a_1)/2$, $q_0 = 1/d$, $Q = 20q_0$, $q' = (q - Q)/q_0$.

The diffraction amplitude for a GaAs layer is exactly:

$$\hat{\mu}_0(q) = \left[f_{Ga}(q)e^{i\pi q a_0/2} + f_{As}(q)\right] e^{-i\pi q n_0 a_0} \frac{\sin \pi q n_0 a_0}{\sin \pi q a_0/2} = \hat{T}_0(q) \tag{10}$$

and similarly for the AlAs layer

$$\hat{\mu}_1(q) = \left(f_{Al}(q)e^{i\pi q a_1/2} + f_{As}(q)\right) e^{-i\pi q n_1 a_1} \frac{\sin \pi q n_1 a_1}{\sin \pi q a_1/2} = \hat{S}_0(q) \tag{11}$$

They are the two building blocks of the spectrum. As has been done by other authors (see, e.g. [20, 21]), let us define as $\hat{S}_n(q)$ the diffraction amplitude for a heterostructure of length $L = 2^n d$ when the generating Thue-Morse chain is built with initial conditions $\varepsilon_0 = 1$ and $T_n(q)$ as the corresponding amplitude when the initial condition is $\varepsilon_0 = 0$ ("mirror chain"), that is $\hat{S}_0(q) = \hat{\mu}_1(q)$, $\hat{T}_0(q) = \hat{\mu}_0(q)$.

For a Prouhet-Thue-Morse heterostructure of length $L = 2d$ the sequence is (1, 0) and the amplitude is

$$\hat{S}_1(q) = \hat{\mu}_1(q) + e^{-2i\pi q d_1}\hat{\mu}_0(q) \tag{12}$$

For the "conjugate" or "mirror" chain (0, 1)

$$\hat{T}_1(q) = \hat{\mu}_0(q) + e^{-2i\pi q d_0}\hat{\mu}_1(q) \tag{13}$$

Similarly

$$\begin{aligned} \hat{S}_2(q) &= \hat{S}_1(q) + e^{-4i\pi q d}\,\hat{T}_1(q) \\ \hat{T}_2(q) &= \hat{T}_1(q) + e^{-4i\pi q d}\,\hat{S}_1(q) \end{aligned} \tag{14}$$

and with $\omega = e^{-2i\pi q d} = e^{-2i\pi q'}$

$$\begin{aligned} \hat{S}_{n+1}(q) &= \hat{S}_n(q) + \omega^{2^n}\hat{T}_n(q) \\ \hat{T}_{n+1}(q) &= \hat{T}_n(q) + \omega^{2^n}\hat{S}_n(q) \end{aligned} \tag{15}$$

$$\begin{pmatrix} \hat{S}_n(q) \\ \hat{T}_n(q) \end{pmatrix} = \prod_{1 \le j < n} \begin{pmatrix} 1 & \omega^{2^j} \\ \omega^{2^j} & 1 \end{pmatrix} \begin{pmatrix} \hat{S}_1(q) \\ \hat{T}_1(q) \end{pmatrix} = M_{n-1}(\omega^2) \begin{pmatrix} \hat{S}_1(q) \\ \hat{T}_1(q) \end{pmatrix} \tag{16}$$

which easily yields, for a PTM heterostructure of length $L = 2^n d$ the general formula for the diffraction amplitude:

$$\begin{aligned} &\hat{S}_n(q) = \\ &2^{n-1}\exp\left(-i\pi q \frac{n_0 a_0 + n_1 a_1}{2}\left(2^{n-1}+1\right)\right)\Bigg\{ \left[\left(f_{Ga}(q)e^{i\pi q a_0/2} + f_{As}(q)\right)\frac{\sin \pi q n_0 a_0 \cos \pi q n_1 a_1}{\sin \pi q a_0/2}\right. \\ &\left. + \left(f_{Al}(q)e^{i\pi q a_1/2} + f_{As}(q)\right)\frac{\sin \pi q n_1 a_1 \cos \pi q n_0 a_0}{\sin \pi q a_1/2}\right] \times \prod_{j=1}^{n-1} \cos\left(2^j \pi q \frac{(n_1 a_1 + n_0 a_0)}{2}\right) \\ &-(-i)^n \left[\left(f_{Ga}(q)e^{i\pi q a_0/2} + f_{As}(q)\right)\frac{\sin \pi q n_0 a_0 \sin \pi q n_1 a_1}{\sin \pi q a_0/2}\right. \\ &\left. - \left(f_{Al}(q)e^{i\pi q a_1/2} + f_{As}(q)\right)\frac{\sin \pi q n_1 a_1 \sin \pi q n_0 a_0}{\sin \pi q a_1/2}\right] \times \prod_{j=1}^{n-1} \sin\left(2^j \pi q \frac{(n_1 a_1 + n_0 a_0)}{2}\right)\Bigg\} \end{aligned} \tag{17}$$

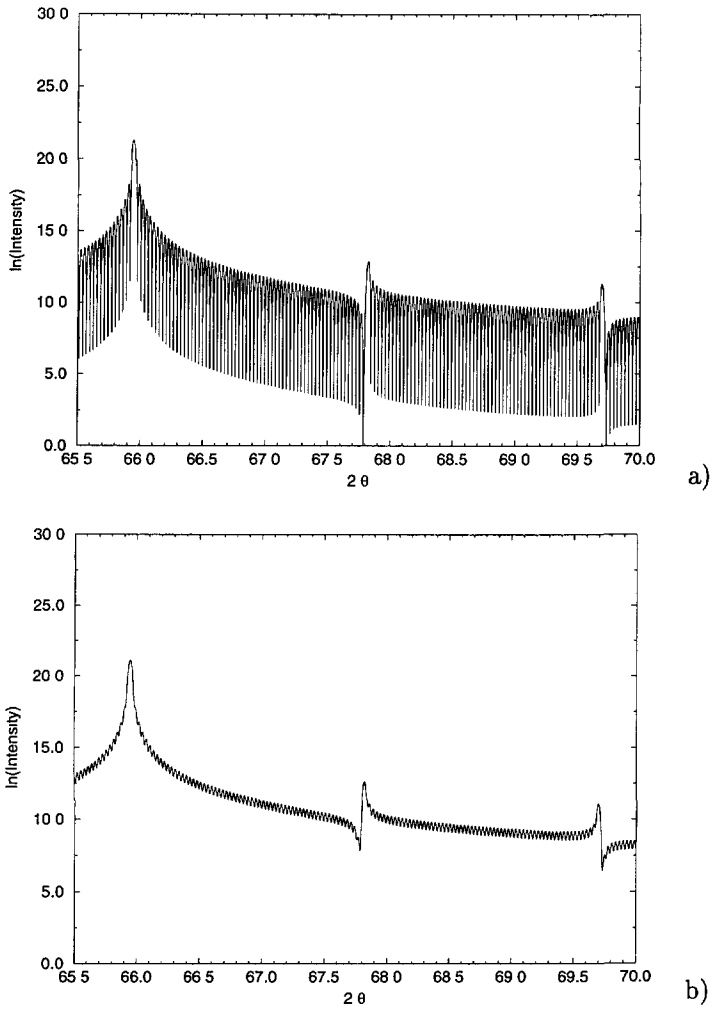

Fig. 1. — Square modulus of the "cosine term" of equation (17) (logarithmic scale) for $n = 7$ ($N = 2^7$ layers) *versus* 2θ and q': (a) without detector slit width, (b) with a detector slit width of 0.0173° as defined in the text.

The intensity is then trivially

$$I_n(q) = \left|\hat{S}_n(q)\right|^2 = \hat{S}_n^*(q)\hat{S}_n(q) \tag{18}$$

For simplicity we rewrite $\hat{S}_n(q)$, for the investigated sample having $d_0 = 5a_0$ and $d_1 = 5a_1$ since $n_0 = n_1 = 5$

$$\hat{S}_n(q) = 2^{n-1}\mathrm{e}^{\imath\psi_n(q)}\left\{(F_0(q)C_0(q) + F_1(q)C_1(q))\prod_{j=1}^{n-1}\cos\left(2^j\pi q\frac{5\,(a_1+a_0)}{2}\right)\right.$$
$$\left.-(-i)^n\,(F_0(q)D_0(q) - F_1(q)D_1(q))\prod_{j=1}^{n-1}\sin\left(2^j\pi q\frac{5\,(a_1+a_0)}{2}\right)\right\} \tag{19}$$

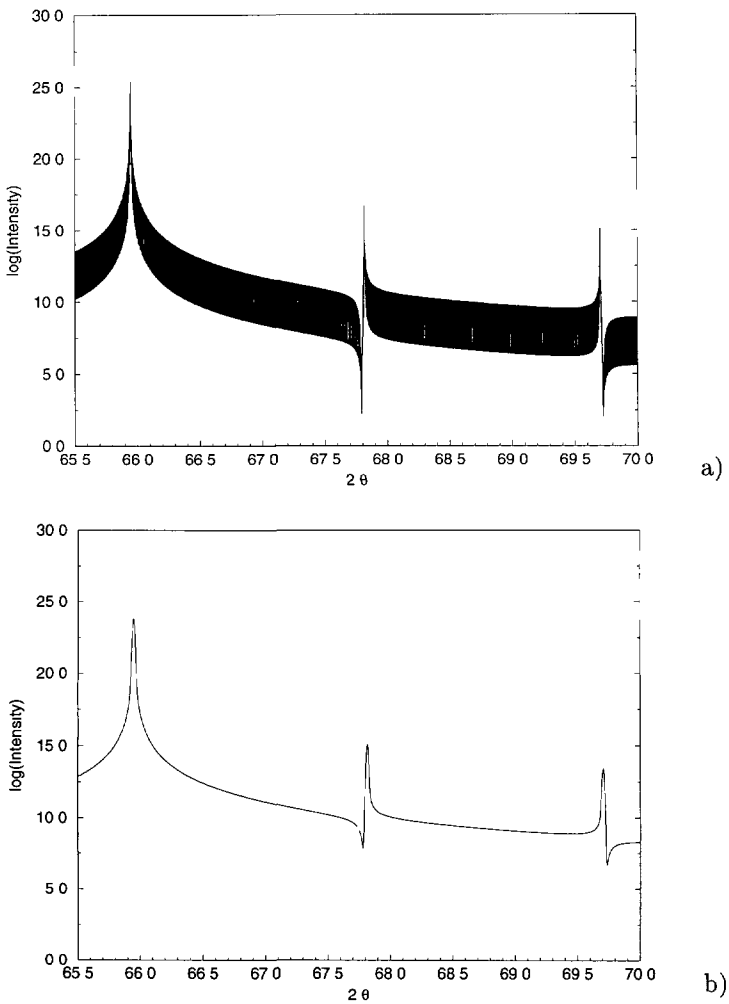

Fig. 2. — Same as Figure 1 for $n = 10$ ($N = 2^{10}$ layers).

The exponents $\alpha_n(q)$ characterizing peak intensity dependence on sample size n, with $L = 2^n d$, and wave vector q are defined by

$$I_n(q) = I_0(q) 2^{n\alpha_n(q)} \tag{20}$$

We first note that, because of the values of the two different atomic structure factors $f_{\mathrm{Ga}}(q)$ and $f_{\mathrm{Al}}(q)$, one can *never* have $|F_0(q)| = |F_1(q)|$ even if $a_1 = a_0$ [24, 25].

We restrict, without loss of generality, our analysis to the range $66° < 2\theta < 70°$ (See Fig. 1 of [1]). In the published high resolution experimental spectra (Figs. 2 and 3 of [1], our Figs. 5c and 6c) one first observes two sharp peaks near $2\theta = 66°$. One is the 004 peak of the GaAs multilayer substrate. In these spectra, q runs from $20q_0$ to $21q_0$, approximately, therefore q' runs from 0 to 1. The second sharp peak corresponds to the value $q = Q = 20q_0$. We measure $2\theta = 66.052°$ for the GaAs 004 peak ($q = 4/a_0$) and $2\theta = 65.944°$ for the $q = Q = 20q_0$ peak from these figures and we get $a_0 = 5.653$ Å for GaAs, and $a_1 = 5.669$ Å for AlAs. There is a

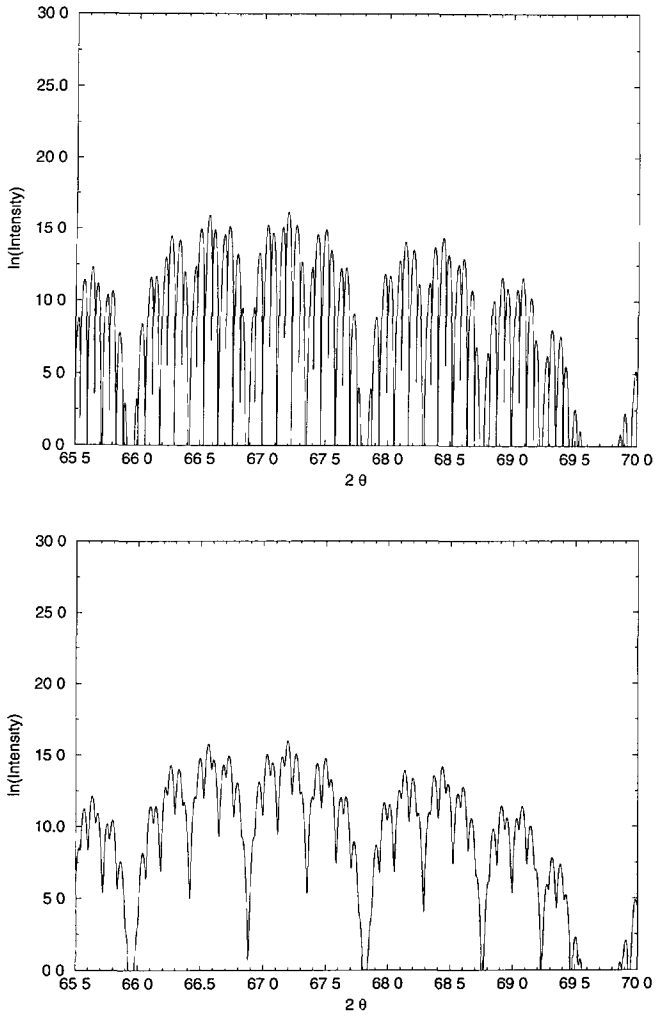

Fig. 3. — Square modulus of the "sine term" of equation (17) (logarithmic scale) for $n = 7$ ($N = 2^7$ layers) *versus* 2θ and q': (a) without detector slit width, (b) with a detector slit width of 0.0173° as defined in the text.

significant discrepancy between our value of a_1 and the AlAs lattice constant in the literature [22], which may be due to the effects of alternating AlAs with GaAs. We use our values for a_0 and a_1 throughout the numerical computations of this work (see Figures), in order to compensate for the fact that we work with a two-length model as indicated above.

In the conditions of the experiment, the X-ray spectrum is recorded using a detector with a finite slit width which we must take into account when we calculate the spectrum from equation (18). In other words, it means that to accurately describe the experimental situation we must *average* the data $I_n(q')$ we obtain from the computer (with q' taken from the mesh used in the interval $0 \leq q' < 1$) over the detector width. This very important and relevant step allows one to bridge the gap between the abstract mathematical formula and the real physical system. In particular, we simulate the detector window in the numerical calculation by convoluting the

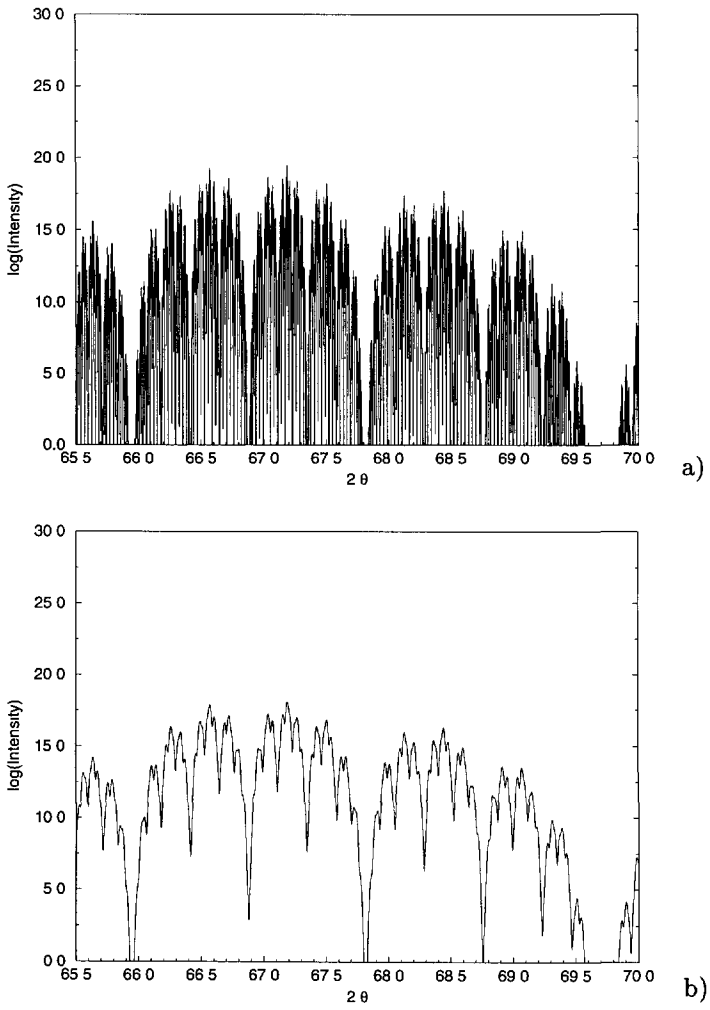

Fig. 4. — Same as Figure 3, for $n = 10$ ($N = 2^{10}$ layers).

calculated intensity with a Gaussian whose width in 2θ at half maximum height is 0.0173°.

The structure factors $F_0(q)$ and $F_1(q)$ are essentially constant over the range of values of θ studied. They are described in the numerical calculation using the algorithm of chapter 2.2 of reference [23]. The phase relationship between adjacent planes of atoms also does not vary more than about $\pi/10$ over this range. This would no longer be true if the spectrum were calculated over a larger range of q (see Fig. 1 of [1]).

Let us now analyse separately the behaviour of the two terms in equation (19), which, for the sake of simplicity, we hereafter denote "cosine term" the first term, and "sine term" the second.

The square modulus of the "cosine term" is plotted in Figures 1a and b, and 2a and b without and with averaging over the detector width for $n = 7$ and $n = 10$ ($N = 2^7$ and $N = 2^{10}$). It clearly appears that this contribution is roughly independent of sample size n, except in the

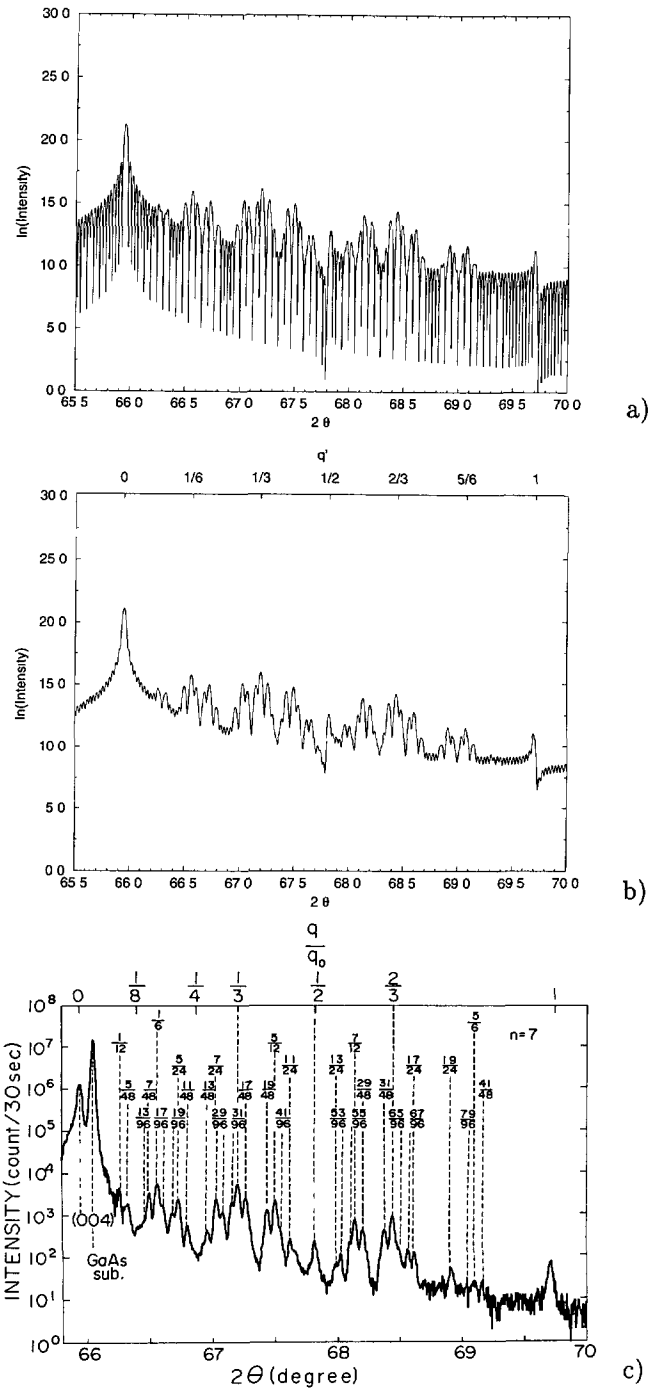

Fig. 5. — a) Total intensity of the high resolution PTM X-ray diffraction pattern (logarithmic scale) for $n = 7$ ($N = 2^7$ layers) *versus* 2θ and q', without detector slit width. b) Total intensity of the high resolution X-ray diffraction pattern for $n = 7$ ($N = 2^7$ layers) with a detector slit width of 0.0173° as defined in the text. c) Experimental spectrum (Reprinted with permission from *Phys. Rev. Lett.* **66** (1991) 2223. Copyright 1991 The American Physical Society).

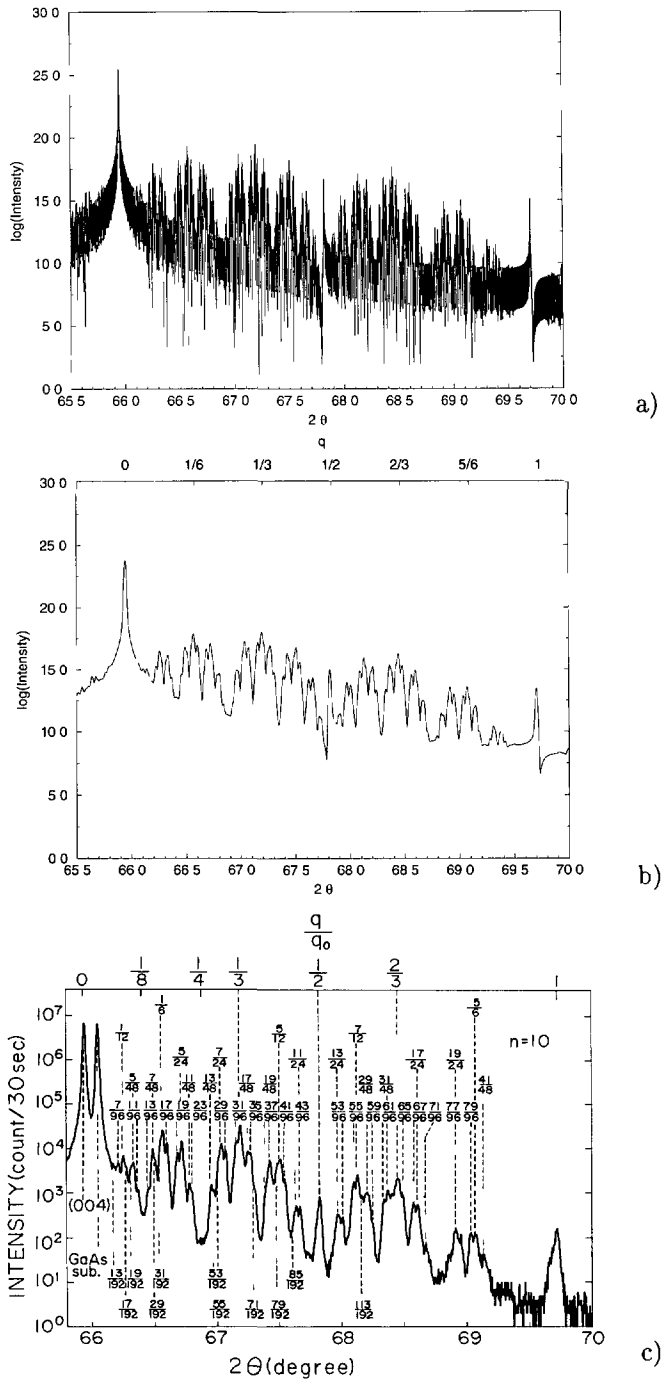

Fig. 6. — Same as Figure 5 for $n = 10$ ($N = 2^{10}$ layers).

immediate vicinity of $q' = 0$, $1/2$ and 1. Therefore, in most of the spectrum in the conditions of the experiment this term can be neglected with respect to the second. The peaks at $q' = 1/2$ and 1 are isolated "Dirac type" peaks, about which we comment more later on (see Sect. 5),

of the kind which appear in the calculation of the Fourier Transform of the abstract PTM sequence when the alphabet is changed from (1, −1) to (1, 0) [12]. The bare value of $\alpha_n(q)$ for these peaks is of course 2. Note that the peaks at $q' = 1/2$ and 1 vanish in the special case where $a_0 = a_1 = a$, because the prefactors $C_0(q)$ and $C_1(q)$ are then identically zero, at these values of q'.

The "sine term" carries the singular continuous characteristics of the spectrum. Its square modulus is plotted in Figures 3a and b, and 4a and b without and with averaging over the detector width for $n = 7$ and $n = 10$. The prefactor $F_0(q)D_0(q) - F_1(q)D_1(q)$ has observable effects on the diffraction amplitudes. Here, q runs from $20q_0$ to $21q_0$, and since $a_0 \simeq a_1$, the sine factor in $F_0(q)D_0(q) - F_1(q)D_1(q)$ vanishes at two values of q in the vicinity of $q = 21q_0$, leading to a suppression of the peaks which is well visible in this region of the experimental spectra, especially in the $n = 7$ case, and well reproduced in our calculations. Around $q = 20q_0$, the $F_0(q)D_0(q) - F_1(q)D_1(q)$ prefactor does not vanish because the denominators and numerators of $D_0(q)$ and $D_1(q)$ both go to zero at $q = 4/a_0$ and $4/a_1$, so that the limit is not zero in this case.

Since its prefactor $F_0(q)D_0(q) - F_1(q)D_1(q)$, - which acts roughly as a coarse modulation, - does not depend on sample size n, and the first term is negligible when q belongs to the support of the second, the main contribution to the exponents $\alpha_n(q)$ comes from the sine product alone, from which they can be well estimated [1].

For the same reasons, the peaks of the "singular continuous part" of the spectrum are in fact generated by the sine product. It is obvious that this product is zero for $q' = \ell/2^p$, ℓ and p integers. Rolle's theorem then shows that there is at least one cancellation of its derivative, (one extremum, or a maximum of intensity) between each zero. Then considerations of degree on relevant polynomials show that there is only one on each open interval between zeros. For sample size n then, there are 2^{n-1} peaks, and these peaks are well labelled indeed by the irreducible rationals $k/(3.2^m)$, k and m integers with $n - 2$ as an upper bound on m and a precision of about 10^{-3}, which agrees very well with the experimental precision announced in [1], (better than 5×10^{-3}). Since the sample has finite size, *there are no other peaks* [24, 25].

The effects of finite detector slit width is most apparent in the case where the slit width is larger than the peak width. Then the peak intensity calculated from equation (18) can no longer be directly observed because of the effects of the integration of intensity and the "shouldering" of close peaks, and a careful deconvolution and a subtraction of the background must be done as indicated in [1] in order to perform peak assignment and measurement of $\alpha_n(q)$ from the spectra. However, in the present case, the inevitable presence of the detector width does not prevent the exact characterization of the nature of the spectrum, or a sufficiently faithful measurement of its principal characteristics, at variance with what is found in the Rudin-Shapiro situation [26]. The total intensity is shown in Figures 5 and 6.

5. Effects of Layer Surface Roughness

We now must take into account the unavoidable existence of layer surface roughness in the Molecular Beam Epitaxy made heterostructure sample. We emphasize that only the diffraction pattern along a direction normal to the layers is calculated, which involves the Fourier Transform of the projection of the structure onto a line normal to the planes. Roughness affects the projection in two ways:

1) there are fluctuations in the thickness of individual GaAs (AlAs) layers,
2) there are regions that, due to the projection are seen as a "mixture" of GaAs and AlAs.

As an approximation, we ignore factor 2) and represent roughness simply by a random variation in thickness of both kinds of layers as follows.

Let $\{\delta_j\}_{j\geq 0}$ be a sequence of symmetric, independent, and identically distributed random variables with values between -1 and 1. Their common characteristic function is denoted by φ:

$$\varphi(t) = E\left(e^{2i\pi t\delta}\right) \tag{21}$$

where E stands for the expectation or mean value.

We consider two lengths a_1 and a_{-1}, and a chain of two kinds of "atoms", whose succession follows the PTM sequence and the abscissa of the j th "atom" is so defined:

$$\begin{aligned} \ell_0 &= 0 \\ \ell_{j+1} &= \ell_j + a_{\varepsilon_j}(1+\delta_j) \end{aligned}$$

Setting the lattice spacings to

$$\begin{aligned} a_1 + a_{-1} &= 2 \\ a_1 - a_{-1} &= 2\tau \end{aligned} \tag{22}$$

we have, for the chain length from the origin to site j is ℓ_j

$$\ell_j = \frac{j+s_j}{2}a_1 + \frac{j-s_j}{2}a_{-1} + \sum_{0\leq k<j} a_{\varepsilon_k}\delta_k = j + \tau s_j + \Delta_j \tag{23}$$

The Fourier Transform of this simple chain is

$$F_n(q) = \sum_{0\leq j<2^n} \varepsilon_j\, e^{-2i\pi q\ell_j} \tag{24}$$

Then, the expectation value for the corresponding intensity, $E\left(|F_n(q)|^2\right)$

$$\begin{aligned} E\left(|F_n(q)|^2\right) &= \sum_{0\leq j,k<2^n} \varepsilon_j\varepsilon_k\, e^{-2i\pi q(j-k+\tau(s_j-s_k))} E\left(e^{-2i\pi q(\Delta_j-\Delta_k)}\right) \\ &= \sum_{0\leq j,k<2^n} \varepsilon_j\varepsilon_k\, e^{-2i\pi q(j-k+\tau(s_j-s_k))} \varphi(q\,a_1)^{|(j+s_j-k-s_k)/2|}\, \varphi(q\,a_{-1})^{|(j-s_j-k+s_k)/2|} \end{aligned} \tag{25}$$

To emphasize the dependence on a_1 and a_{-1}, let us set $E\left(|F_n(q)|^2\right) = S_n(a_1, a_{-1})$, with, obviously, $S_0(a_1, a_{-1}) = 1$. For $n \geq 0$ we have the following recursion formula:

$$\begin{aligned} &S_{n+1}(a_1, a_{-1}) = S_n(a_1, a_{-1}) + S_n(a_{-1}, a_1) \\ &- \sum_{0\leq j,k<2^n} \varepsilon_j\varepsilon_k\, e^{-2i\pi q[2^n+j-k+\tau(-s_j-s_k)]} \sqrt{\varphi(q\,a_1)}^{(2^n+j-k-s_j-s_k)} \sqrt{\varphi(q\,a_{-1})}^{(2^n+j-k+s_j+s_k)} \\ &- \sum_{0\leq j,k<2^n} \varepsilon_j\varepsilon_k\, e^{-2i\pi q[-2^n+j-k+\tau(s_j+s_k)]} \sqrt{\varphi(q\,a_1)}^{(2^n+k-j-s_j-s_k)} \sqrt{\varphi(q\,a_{-1})}^{(2^n+k-j+s_j+s_k)} \end{aligned} \tag{26}$$

One defines:

$$\begin{aligned} \alpha &= \sqrt{\varphi(q\ a_1)\,\varphi(q\ a_{-1})} \\ \rho &= \sqrt{\frac{\varphi(q\ a_{-1})}{\varphi(q\ a_1)}} \\ z &= \alpha\ \mathrm{e}^{-2\imath\pi q} \\ w &= \rho\ \mathrm{e}^{2\imath\pi q\tau} \end{aligned} \tag{27}$$

In the calculations, we used the following law for variables: each assumes the value 0 with probability $1-2p$, and values $+$ or $-\beta$ each with probability p. The meaning of these two parameters is the following. The parameter β corresponds to the variation in the number of layers deposited and the parameter $2p$ is the probability that a specific layer be disturbed.

One can notice that the existence of the subsequent recursion relation (30) allows one to make, for each q, an accurate computation of $E\left(|F_n(q)|^2\right)$; this is why we have considered this model, although it is not the exact "randomization" of the diffraction amplitude calculation. But it is an excellent approximation, due to the fact that, as we have shown before, the prefactors $F_0(q)C_0(q) + F_1(q)C_1(q)$ and $F_0(q)D_0(q) - F_1(q)D_1(q)$ of formula (19) are smooth in q and do not depend on sample size n, therefore, they do not contribute to the exponents $\alpha_n(q)$.

Then, also for $n \geq 0$, and writing now $S_n(\tau)$ instead of $S_n(a_1, a_{-1})$:

$$S_{n+1}(\tau) = S_n(\tau) + S_n(-\tau) - z^{2^n} v_n(z,w)\ v_n\left(\frac{1}{z}, w\right) - \overline{z}^{2^n} v_n(\overline{z}, \overline{w})\ v_n\left(\frac{1}{\overline{z}}, \overline{w}\right) \tag{28}$$

where $\overline{z}$ stands for the complex conjugate of z, and

$$\begin{aligned} v_n(x,w) &= \sum_{0 \leq j < 2^n} \varepsilon_j z^j w^{s_j} \\ &= \left(1 - \frac{z}{2}\left(w + \frac{1}{w}\right)\right) \prod_{1 \leq j < n} \left(1 - z^{2^j}\right) - \frac{z}{2}\left(w - \frac{1}{w}\right) \prod_{1 \leq j < n} \left(1 + z^{2^j}\right) \end{aligned} \tag{29}$$

with $v_0(x,y) = 1$
In other words,

$$S_{n+1}(\tau) = S_n(\tau) + S_n(-\tau) - 2\mathrm{Re}\left[-z^{2^n} v_n(z,w)\ v_n\left(\frac{1}{z}, w\right)\right] \tag{30}$$

The corresponding calculated intensities are shown in Figure 7 for values of q' ranging from 0.47 to 0.501, and for the chain length 2^{14} This parameter region exhibits the 1/2 Dirac type peak as well as other peaks from the "singular continuous" part of the diffraction spectrum. Our results clearly show that, in the intermediate regime - finite sample size *and* small values of p and β, - the $q' = 1/2$ peak is particularly vulnerable to the effects of roughness:. its exponent, starting from the characteristic value of 2, drops more in response to increase of p and β than the exponents of peaks from the "singular continuous" part of the spectrum, like $q' = 1/3$, for example or the peak neighbouring $q' = 1/2$ labelled $91/(3.2^6)$. Upon increase in roughness, both types of exponents will eventually reach 1.

Therefore, the effect of this random variation of layer thickness is to endow the peaks of the diffraction spectrum with glasslike characteristics: a) they are broadened, b) the value of $\alpha_n(q)$

for the Dirac type as well as for the peaks of the "singular continuous" part of the spectrum rapidly converges, even at finite sample size, to the characteristic value of 1.

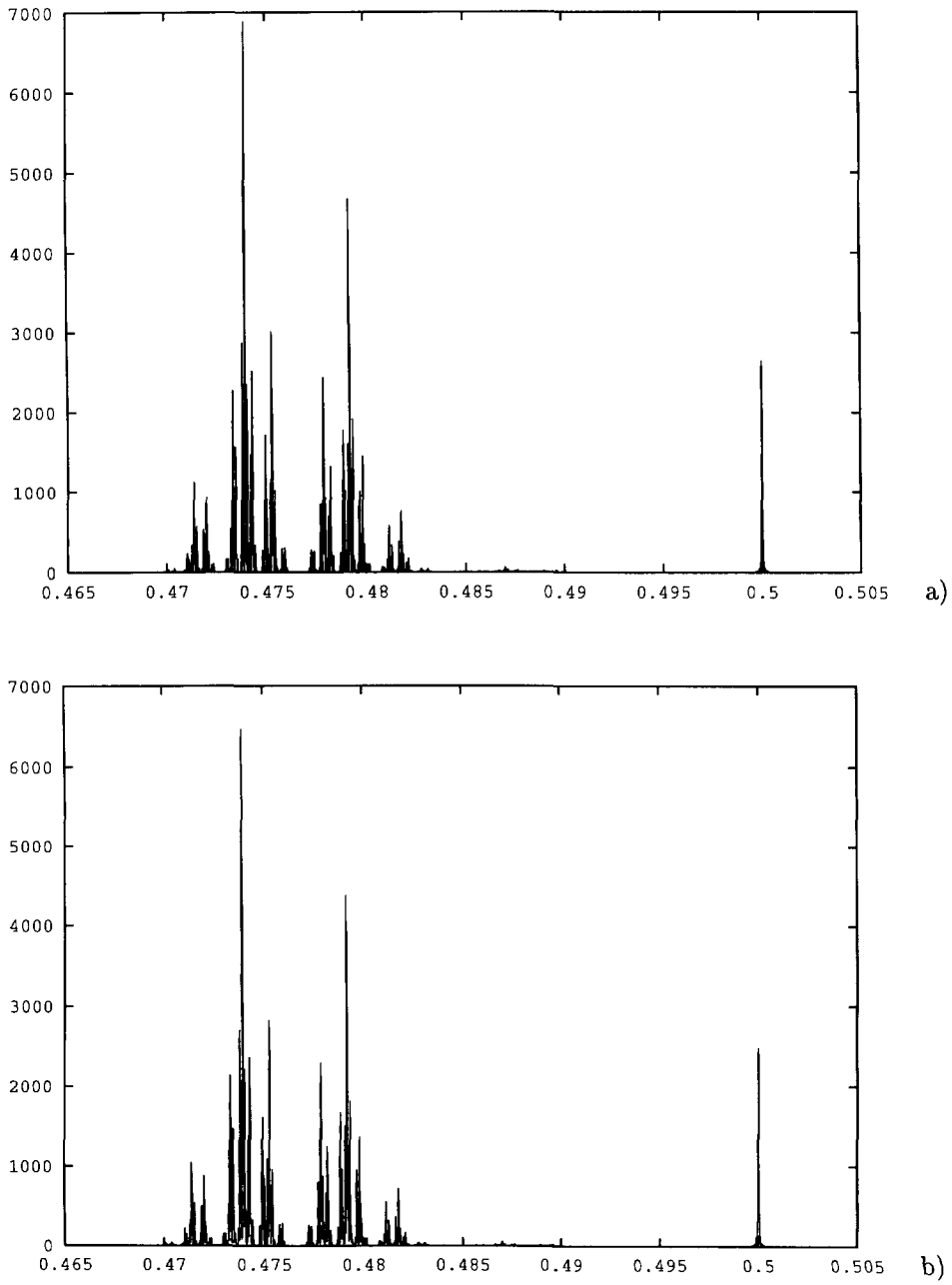

Fig. 7. — Intensity of the PTM X-ray spectrum *versus* q', calculated from equation (30) for q' ranging between 0.47 and 0.501, with a thickness difference $\tau = 0.002$, for $n = 14$ ($N = 2^{14}$ layers): a) with no roughness, $p = 0$ and $\beta = 0$, b) with $p = 0.001$ and $\beta = 0.05$, c) with $p = 0.005$ and $\beta = 0.05$, d) with $p = 0.005$ and $\beta = 0.1$.

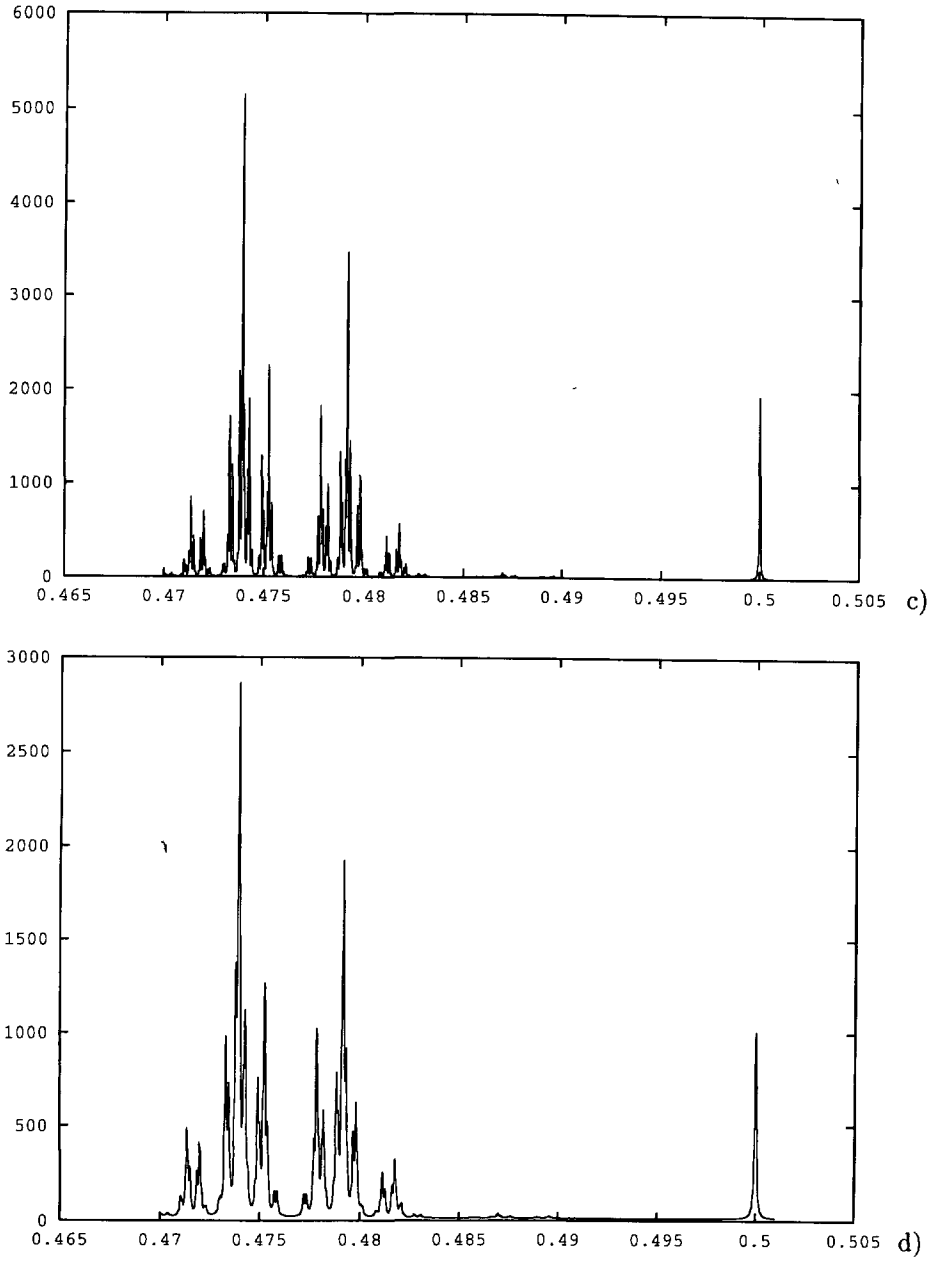

Fig. 7. — *(continued).*

6. Conclusion

We presented a detailed and thorough theoretical and numerical line shape analysis of the previously published [1] high resolution X-ray diffraction spectra of finite size Thue-Morse GaAs-AlAs superlattice heterostructures, which fully confirms the essentials of the preliminary analysis of previous work: most of the peaks are labeled by the irreducible rationals $k/(3.2^m)$ in convenient units, the dependence of their intensity on sample size is gov-

erned by exponents $\alpha_n(q), 0 < \alpha_n(q) < 2$ and the diffraction spectrum retains the essential properties of a singular continuous measure. The effect of instrumental parameters is taken into account, in particular detector resolution effects. Furthermore we investigated the effects on the diffraction spectrum of Molecular Beam Epitaxy deposited layer roughness, represented by a random fluctuation of layer thickness. We show that roughness endows the diffraction peaks with glasslike characteristics. In the intermediate regime, however, the Dirac type peaks at $q' = 1/2$, for example, are more affected than the peaks from the "singular continuous" part of the spectrum.

Acknowledgments

The authors are pleased to acknowledge stimulating discussions with F. Dénoyer and A. Janner.

References

[1] Axel F., Terauchi H., *Phys. Rev. Lett.* **66** (1991) 2223.

[2] Schechtman D., Blech I., Gratias D. and Cahn J.W., *Phys. Rev. Lett.* **53** (1984) 1951.

[3] Prouhet E., *C. R. Acad. Sci. Paris Sér. I* **33** (1851) 31.

[4] Thue A., *Norske vid. Selsk. Skr. I. Mat. Nat. Kl. Christiania* **7** (1906) 1-22; **13** (1912) 1-67.

[5] Morse M., *Trans. Am. Math. Soc.* **22** (1921) 84-100.

[6] Christol G., Kamae T., Mendès France M. and Rauzy G., *Bull. Soc. Math. France* **108** (1980) 401.

[7] Dekking M., Mendès France M. and van der Poorten A., *Mathematical Intelligencer* **4** (1982) 130-138; **4** (1982) 173-181; **4** (1982) 190-195 (Springer-Verlag).

[8] Allouche J.P., *Expositiones Mathematicæ* **5** (1987) 239.

[9] Axel F., "Incommensurate Structures in Condensed Matter", Proceedings of the Third International Meeting on Quasicrystals, M.J. Yacaman *et al.* Eds. (World Scientific, Singapore, 1990) pp. 243-249.

[10] Mahler K., *J. Math. Phys.* **6** (1927) 158-163.

[11] Kakutani S., "Proceedings of the Sixth Berkeley Symposium on Mathematical Statistics and Probability (Univ. of California Press, California, 1970) Vol. 2, pp. 319-326.

[12] Queffelec M., "Substitution Dynamical Systems - Spectral Analysis", Lecture Notes in Mathematics, vol. 1294 (Springer-Verlag, Berlin, 1987).

[13] Riesz R. and Nagy B.Sz., "Leçons d'Analyse Fonctionnelle" (Gauthiers-Villars, Parius, 1968); see also Rudin W., "Real and Complex Analysis" (McGraw-Hill, New York, 1974).

[14] Merlin R., Bajema K., Clarke R., Juang F.Y. and Bhattacharya P.K., *Phys. Rev. Lett.* **55** (1985) 1768.

[15] Terauchi H., Sekimoto S., Kamigaki K., Sakashita H., Sano N., Kato H. and Nakayama M., *J. Phys. Soc. Jpn* **54** (1985) 4576.

[16] Todd J., Merlin R., Clarke R., Mohanty K.M. and Axe J.D., *Phys. Rev. Lett.* **57** (1986) 1157.

[17] Terauchi H., Noda Y., Kamigaki K., Matsunaka S., Nakayama M., Kato H., Sano N. and Yamada Y., *J. Phys. Soc. Jpn* **57** (1988) 2416.

[18] Terauchi H., Kamigaki K., Okutani T., Nishihata Y., Kasatani H., Kasano H., Sakane K., Kato H. and Sano N., *J. Phys. Soc. Jpn* **59** (1990) 405.

[19] Merlin R., Bajema K., Nagle J. and Ploog K., *J. Phys. Colloq. France* **48** (1987) C5-503-C5-506.

[20] Kolar M., Iochum B., Raymond L., *J. Phys. A: Math. Gen.* **26** (1993) 5489.

[21] Kolar M., *Phys. Rev.* **B47** (1993) 5489.

[22] Donnay J.D.H., "Crystal Data: Determinative Tables", 2nd ed. (American Crystallographic Association, Washington, 1963).

[23] "International Tables for X-ray Crystallography", vol. IV (The Kynoch Press, publ., 1974) pp. 71-99.

[24] Kolar M., *Phys. Rev. Lett. (Comment)* **73** (1994) 1307.

[25] Axel F., Terauchi H., *Phys. Rev. Lett (Reply)* **73** (1994) 1308.

[26] Axel F., Allouche J.P., Wen Z.-Y., *J. Phys. C: Condens. Matter Phys.* **4** (1992) 8713.

[27] Cheng Z., Savit R., Merlin R., *Phys. Rev.* **B37** (1988) 4375.

[28] Cheng Z., Savit R., *J. Stat. Phys.* **60** (1990) 383.

[29] Peyrière J., *Ann. Inst. Fourier, Grenoble* **25** (1975) 127-169.

[30] Godrèche C., Luck J.M., *J. Phys. A: Math. Gen.* **23** (1990) 3769.

[31] Luck J.M., *Phys. Rev.* **B39** (1989) 5834.